arXiv:1408.2577v2 [physics.comp-ph] 27 Aug 2014

Investigating the interplay between mechanisms of anomalous diffusion via fractional Brownian walks on a comb-like structure

Haroldo V. Ribeiro[1,2,3], **Angel A. Tateishi**[4], **Luiz G. A. Alves**[1,3], **Rafael S. Zola**[1,2], **Ervin K. Lenzi**[1,3]

[1]Departamento de Física, Universidade Estadual de Maringá, Maringá, PR 87020-900, Brazil

[2]Departamento de Física, Universidade Tecnológica Federal do Paraná - Apucarana, PR 86812-460, Brazil

[3]National Institute of Science and Technology for Complex Systems, CNPq - Rio de Janeiro, RJ 22290-180, Brazil

[4]Departamento de Física, Universidade Tecnológica Federal do Paraná - Pato Branco, PR 85503-390, Brazil

E-mail: hvr@dfi.uem.br

Abstract. The comb model is a simplified description for anomalous diffusion under geometric constraints. It represents particles spreading out in a two-dimensional space where the motions in the x-direction are allowed only when the y coordinate of the particle is zero. Here, we propose an extension for the comb model via Langevin-like equations driven by fractional Gaussian noises (long-range correlated). By carrying out computer simulations, we show that the correlations in the $y-$direction affect the diffusive behavior in the $x-$direction in a non-trivial fashion, resulting in a quite rich diffusive scenario characterized by usual, superdiffusive or subdiffusive scaling of second moment in the $x-$direction. We further show that the long-range correlations affect the probability distribution of the particle positions in the $x-$direction, making their tails longer when noise in the $y-$direction is persistent and shorter for anti-persistent noise. Our model thus combines and allows the study/analysis of the interplay between different mechanisms of anomalous diffusion (geometric constraints and long-range correlations) and may find direct applications for describing diffusion in complex systems such as living cells.

PACS numbers: 05.40.-a, 87.10.Mn, 89.75.-k, 05.40.Fb

Keywords: anomalous diffusion, comb model, fractional Brownian motion, long-range correlations Submitted to: *New J. Phys.*

1. Introduction

Understanding diffusive motions is a long-standing problem in the physicists' agenda. Since the works of Einstein, Smoluchowski and Langevin, we know that one of the most striking patterns of classical (usual) free diffusion is the linear growth with time of the second moment of the particle positions. While this feature is ubiquitous in nature, many other patterns have been also observed for the second moment, both from analytical calculations and experimental data [1]. These deviants behaviors are often called anomalous diffusion.

Nowadays, efforts have been mainly focused on understanding the underlying physical mechanisms that lead to such deviations, since only the classification of the diffusive behaviors of a given system is not enough to fully characterize it. In this context, two common pathways for anomalous diffusion are long-range correlations in the particle positions and geometric constraints related with the structural complexity of the environment where the particles are moving. The former may be related to memory affects and an example is the fractional Brownian motion [2, 3], where the second moment has a power-law dependence with time, that is, $\langle x^2(t)\rangle \propto t^{2h}$. For this case, the Hurst exponent h classifies the anomalous diffusion in subdiffusion ($0 < h < 1/2$) or superdiffusion ($h > 1/2$) [4, 5] and also recovers usual ($h = 1/2$) and ballistic ($h = 1$) diffusions as limiting cases. Anomalous diffusion due to geometric constraints is well exemplified by the comb model. In this model, diffusive particles walk on a two-dimensional space; however, motions in the x-direction are only allowed when the y coordinate of the particle positions is zero. The result of this simple constraint is a subdiffusive motion (precisely, $\langle x^2(t)\rangle \sim t^{\alpha}$ with $\alpha = 1/2$) and the appearance of a backbone (at $y = 0$) and teeth (along the $y-$axis direction), which were originally proposed to mimic the quasilinear structure and dangling ends of percolation clusters [6, 7, 8].

Mainly due to its simplicity and ability of mimicking diffusive aspects of highly disordered systems, the comb model has been extensively studied and extended by means of analytical calculations [9, 10, 11, 12, 13, 14, 15] and also employed as simplified description of natural phenomena such as cancer proliferation [16, 17], transport of spiny dendrites [18] and diffusion of ultra cold atoms [19, 20]. Moreover, as crowded environments tend to slow down the diffusive motion of particles by obstruction and/or trapping [21], the comb model could also be used as a toy model for describing diffusion in intracellular processes, where several researchers have reported the existence of subdiffusion and ergodicity breaking in the random walk of different biochemical compounds [22, 23, 24, 25, 27, 26, 28, 21, 29, 30, 31, 32] by using single particle tracking [33]. In the case of intracellular processes, the power-law exponents α describing the second moment ranges from $\alpha \approx 0.1$ to $\alpha \approx 0.9$ (evaluated both from ensemble and time average) and, in the case of ultra cold atoms, α appears as a function of lattice depth and assumes values larger than one ($\alpha > 1$, superdiffusion).

In addition to the anomalous scaling of the second moment, the work of Weiss [34]

has also shown that the diffusive processes of intracellular fluids may present long-range corrections as in the fractional Brownian motion, an empirical finding that have not been explored within the comb model framework. Also, recently, Yamamoto *et al.* [35] have provided evidence (from molecular dynamics simulation) that the anomalous diffusion of water molecules on cell membrane surface arises from both divergent mean trapping time and long-range correlated noises. Here, we extend the comb model by considering a Langevin-like equation where the noises are long-range correlated. Our model thus combines two of the main mechanisms of anomalous diffusion: geometric constraints and long-range correlations, allowing a more complete description of complex diffusive motions and also the study of the interplay between these two mechanisms. By carrying out computer simulations, we show that the correlations in the $y-$direction affect the diffusive behavior in the $x-$direction in a non-trivial fashion and that a quite rich diffusive scenario emerges from these long-range correlations. We report that diffusive process in the $x-$direction of this generalized version of the comb model can be usual, superdiffusive or subdiffusive, depending on both corrections in the x and y directions. We further show that the long-range correlations affect the probability distribution of the particle positions in the $x-$direction: the distribution becomes more leptokurtic when the noise in the $y-$direction is persistent whereas, for anti-persistent noise, it becomes less leptokurtic and approaches the Gaussian distribution as a limiting case.

2. Generalized comb and long-range correlations

We start by writing the generalized diffusion equation describing the motion under the comb structure [36]:

$$\frac{\partial}{\partial t}\rho(x,y;t) = \delta(y) D_x \frac{\partial^2}{\partial x^2}\rho(x,y;t) + D_y \frac{\partial^2}{\partial y^2}\rho(x,y;t)\,, \tag{1}$$

here $\rho(x,y;t)$ is the joint probability of the particle positions (x and y coordinates) as a function of time t, D_x and D_y are the diffusive coefficients in the x and y directions. Note the presence of the Dirac delta $\delta(y)$ multiplying the spatial derivative with respect to x and, consequently, limiting the diffusion in the $x-$direction only for $y = 0$. In order to investigate the role of long-range correlations in this diffusive process, we propose to numerically solve the following coupled Langevin-like equations

$$\begin{aligned} x(t+dt) &= x(t) + \beta_x\, \delta(y)\eta_x(t) \\ y(t+dt) &= y(t) + \beta_y\, \eta_y(t)\,, \end{aligned} \tag{2}$$

where β_x and β_y are constants related to D_x and D_y, $\eta_x(t)$ and $\eta_y(t)$ are fractional Gaussian noises [2, 3], both with zero mean ($\langle\eta_x(t)\rangle = 0$ and $\langle\eta_y(t)\rangle = 0$), unitary variances ($\langle\eta_x^2(t)\rangle = 1$ and $\langle\eta_y^2(t)\rangle = 1$) and correlations functions (for $t_1 \neq t_2$) given by

$$\begin{aligned} &\langle\eta_x(t_1)\,\eta_x(t_2)\rangle \sim h_x(2h_x-1)|t_1-t_2|^{2h_x-1} \quad \text{and} \\ &\langle\eta_y(t_1)\,\eta_y(t_2)\rangle \sim h_y(2h_y-1)|t_1-t_2|^{2h_y-1}\,. \end{aligned} \tag{3}$$

Notice that the noises $\eta_x(t)$ and $\eta_y(t)$ are power-law correlated with scaling exponents $(2h_x-1)$ and $(2h_y-1)$, where h_x and h_y are the so-called Hurst exponents. For $h_{x,y} < 1/2$, the correlation functions have negative signs and the noises are anti-persistent, meaning that positive values are followed by negative values (or vice-versa) more frequently than by chance; while for $h_{x,y} > 1/2$ the correlations are positive, meaning that positive values are followed by positive values and negative values are followed by negative values more frequently than by chance. Fully persistent noises occur as a limiting case when $h_{x,y} = 1$, whereas normal Brownian (white) noises correspond to the limit of $h_{x,y} = 1/2$.

When running out the simulations of the Langevin equations, we have considered a narrow band of thickness ε along the $x-$axis, inside which the diffusion in the $x-$direction occurs. This strip mimics the effect of the Dirac delta $\delta(y)$ (that appears multiplying the noise $\eta_x(t)$ in Eq. 2) and we have verified that the value ε has no influence in the diffusive process, as long as ε and noises amplitudes β_x and β_y are of the same order of magnitude. This restriction ensures that the variable y presents no dynamics inside the strip. For our proposes, we have fixed $\varepsilon = \beta_x = \beta_y = 0.1$. The fractional Gaussian noises $\eta_x(t)$ and $\eta_y(t)$ were generated by following the Hosking method [37]. Figure 1 shows examples of simulated trajectories for three different values of h_y and keeping $h_x = 0.5$. By visual inspection, we note that depending on whether the motion in y is anti-persistent [Fig 1(a)] or persistent [Fig 1(c)], the diffusive behavior in the $x-$direction drastically changes. The anti-persistence in $y(t)$ causes the particle to return more often to the strip where the diffusive motion in the $x-$direction is allowed; consequently, $x(t)$ covers a larger interval along the $x-$axis when compared with the usual comb [$h_x = h_y = 0.5$, Fig 1(b)]. On the other hand, persistence in $y(t)$ causes the particle to return less often to the strip and, consequently, $x(t)$ covers a small interval along the $x-$axis.

Before quantifing the effects of the long-range correlations on the variances of $x(t)$ and $y(t)$, we have first verified whether the Langevin equations [Eq. (2)] are actually equivalent to the generalized diffusion equation [Eq. (1)] when the noises $\eta_x(t)$ and $\eta_y(t)$ are uncorrelated ($h_x = h_y = 0.5$). We thus simulate an ensemble of 10^5 particle positions considering $dt = 1$ and $h_x = h_y = 0.5$. By using these data, we evaluate the temporal evolution of the variances

$$\sigma_x^2(t) = \langle (x(t) - \langle x(t) \rangle)^2 \rangle \quad \text{and}$$
$$\sigma_y^2(t) = \langle (y(t) - \langle y(t) \rangle)^2 \rangle \,, \tag{4}$$

where $\langle \dots \rangle$ denotes ensemble average. Figures 2(a) and (b) show the behavior of $\sigma_x^2(t)$ and $\sigma_y^2(t)$ versus time for several values of the maximum integration time $t_{\max}$ in the Langevin equations, ranging from 2^7 to 2^{14} as indicated in these plots. In both cases, we note a finite-size-like effect characterized by a crossover time $t_\times$ where $\sigma_x^2(t)$ and $\sigma_y^2(t)$ change their behaviors. Despite that and also discarding an initial transient regime ($t \lesssim 10$), we observe that the variance profiles of $\sigma_x^2(t)$ and $\sigma_y^2(t)$ are in well agreement with the power laws predicted by the generalized diffusion equation of the usual comb [Eq. (1)], that is, $\sigma_x^2(t) \sim t^{\alpha_x}$ and $\sigma_y^2(t) \sim t^{\alpha_y}$ with $\alpha_x = 0.5$ and $\alpha_y = 1$ [36, 38, 39]. We have also analyzed the behavior of the crossover time $t_\times$ in function of the maximum

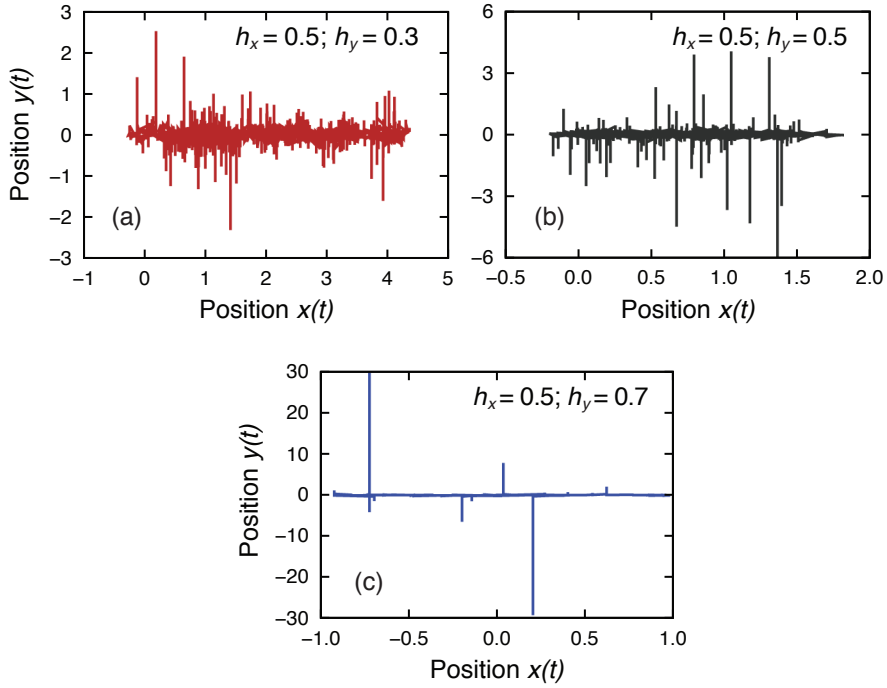

Figure 1. (color online) Simulation of the comb model via a Langevin equation. Examples of simulated trajectories from the generalized comb model described by Eq. 2 with $\varepsilon = \beta_x = \beta_y = 0.1$. We have kept $h_x = 0.5$ and considered three values of the Hurst exponent h_y: (a) $h_y = 0.3$, (b) $h_y = 0.5$ and (c) $h_y = 0.7$. Note that the walker returns less often to $y \approx 0$ when the noise is persistent in the y-direction ($h_y > 0.5$); whereas, for an anti-persistent noise ($h_y < 0.5$), the walker returns more often to $y \approx 0$ when compared with the usual comb ($h_x = h_y = 0.5$).

integration time $t_{\max}$. Figures 2(c) and (d) show that $t_\times$ grows linearly with $t_{\max}$ for $\sigma_x^2(t)$ and $\sigma_y^2(t)$, confirming that the simulated power-law regimes prevail when $t_{\max}$ tends to infinity.

In order to further strengthen the equivalence between our Langevin equations (2) and the diffusion equation (1), we have also evaluated the marginal probability functions $P(x;t) = \int \rho(x,y;t)dy$ and $P(y;t) = \int \rho(x,y;t)dx$ from the simulated data. Figures 3(a) and 3(b) show these distributions for several values of t where we note the spreading of these distributions. For a better comparison with the analytical predictions of Eq. (1), we have also calculated the marginal distributions considering the normalized positions $\xi_x = [x(t) - \langle x(t)\rangle]/\sigma_x(t)$ and $\xi_y = [y(t) - \langle y(t)\rangle]/\sigma_y(t)$. Figures 3(c) and 3(d) reveal a good collapse of the empirical distributions and also a good agreement with the analytical distributions (dashed lines) predicted by Eq. (1), which is a standard Gaussian for $P(\xi_y)$ and can be expressed in terms of the Fox H function for $P(x;t)$ [36, 38, 39] or by the following summation [5, 30]

$$P(\xi_x) = \frac{1}{\pi^{1/4}} \sum_{n=0}^{\infty} \frac{(-1)^n}{n!\,\Gamma[1-(n+1)/4]} \left(\frac{\xi_x^2}{\sqrt{\pi}/4}\right)^{n/2}. \tag{5}$$

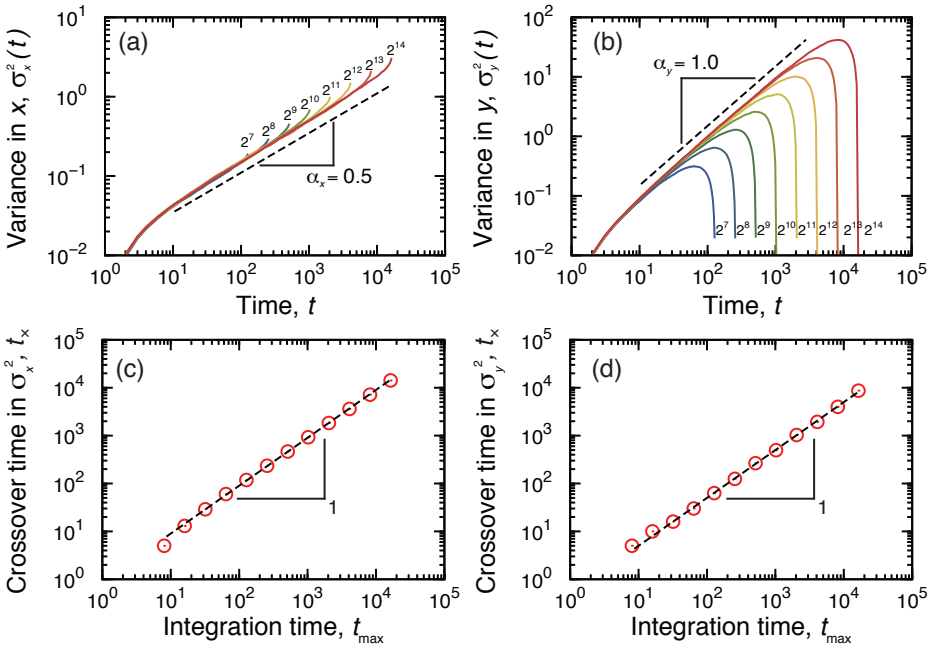

Figure 2. (color online) Equivalence between the variances simulated via the Langevin equations and the analytical results obtained from the generalized diffusion equation in the usual case. Temporal dependence of the variances (a) $\sigma_x^2(t)$ in the x–direction and (b) $\sigma_y^2(t)$ in the y–direction for several values of the maximum integration time $t_{\rm max}$ (as indicated in the plots). The dashed lines represent the predictions of the generalized diffusion equation, that is, $\sigma_x^2(t) \sim t^{\alpha_x}$ with $\alpha_x = 0.5$ and $\sigma_y^2(t) \sim t^{\alpha_y}$ with $\alpha_y = 1$ [36, 38, 39]. We note a finite-size-like effect in both plots. In (c) and (d), we show the crossover time $t_\times$, where the variances $\sigma_x^2(t)$ and $\sigma_y^2(t)$ start to change their behaviors, as a function of the maximum integration time $t_{\rm max}$. We observe that $t_\times$ grows linearly with $t_{\rm max}$ in both cases; therefore, in the limit as $t_{\rm max}$ approaches infinity, the power-law regimes must prevail.

Thus, for the case where no correlations are present in the noises $\eta_x(t)$ and $\eta_y(t)$, the results shown in Fig. 3 corroborate with the equivalence between our simulations of the Langevin equations and the diffusion equation for the comb model.

Convinced of the equivalence in the usual case, we now address the role of the long-range correlations on the diffusive properties of a random walker described by our Langevin equations (2). We first investigate how the memory effects in the y–direction modify the diffusion in the x and y directions. In order to do so, we have built an ensemble of 10^5 particle positions considering $dt = 1$ and $h_x = 0.5$ for each one of nineteen values of h_y homogeneously distributed between 0.05 and 0.95. For each value of h_y, we evaluate the temporal evolution of the variances $\sigma_x^2(t)$ and $\sigma_y^2(t)$. Figures 4(a) and 4(b) show the variance profiles in the x and y directions, respectively. In these plots, the dashed lines represent the behavior for the usual comb, that is, when no correlations are present. In the case of $\sigma_x^2(t)$, we note that the more the noise in y is anti-persistent ($h_y < 0.5$), the larger is the power-law exponent α_x describing the behavior of $\sigma_x^2(t)$; in contrast, persistent noise in y slows down the diffusion and decreases the power-law

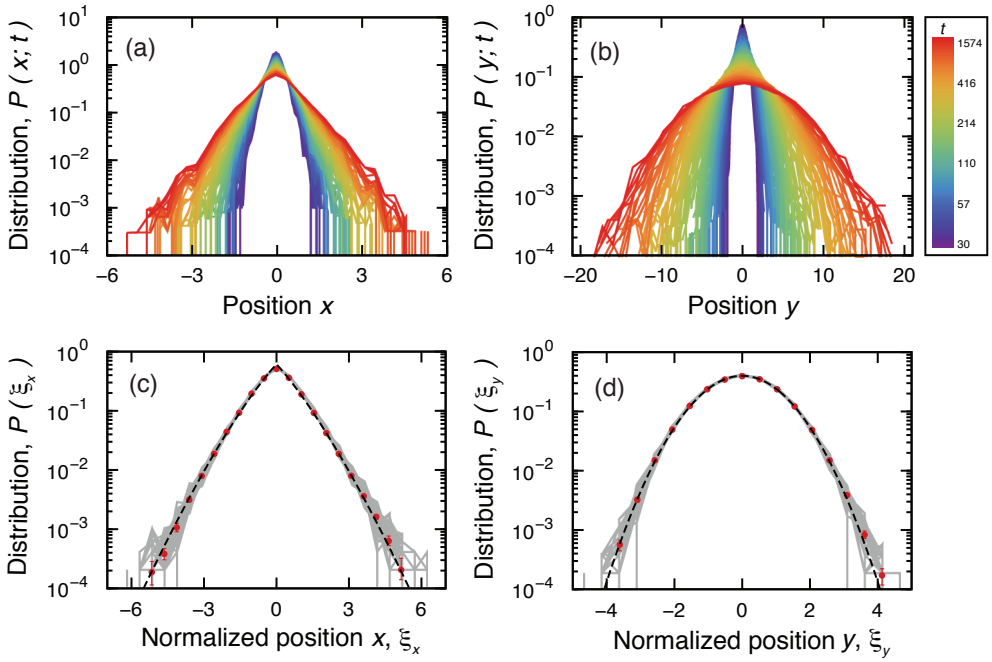

Figure 3. (color online) Equivalence between the marginal distributions $P(x;t)$ and $P(y;t)$ simulated via the Langevin equations and the analytical results obtained from the generalized diffusion equation in the usual case. Marginal distributions (a) $P(x;t)$ and (b) $P(y;t)$ for several values of t, as indicated by color code. We note the spreading of these distributions and the normality of $P(y;t)$. Marginal distributions of normalized positions (c) $P(\xi_x)$ and (d) $P(\xi_y)$ for the same values of t of the previous figures. The gray lines are the marginal distributions for each value of t and the red circles are window average values over all distributions (the error bars are 95% confidence intervals obtained via bootstrapping). The dashed lines are the analytical predictions of Eq. (1); specifically, in (c) the dashed line is the distribution of Eq (5) and in (d) it is the standard Gaussian $P(\xi_y) = (1/\sqrt{2\pi})\exp(-\xi_y^2/2)$. In addition to the good (visual) agreement between simulations and analytical expressions, we have found that the p-values of the Kolmogorov-Smirnov test (testing the equality of the empirical and analytical distributions) are all larger than 0.05, indicating that the hypothesis of the analytical distributions describing our data cannot be rejected at a confidence level of 95%.

exponent α_x. The extreme cases where $h_y = 0.05$ and $h_y = 0.95$ are characterized by $\alpha_x \approx 0.95$ and $\alpha_x \approx 0.19$, respectively. Thus, as we have first noticed in Fig. 1, anti-persistent noise in y forces the walker to return more frequently to the strip where it can move in the $x-$direction and, consequently, the diffusion is enhanced when compared with the case usual comb ($h_y = 0.5$). On the other hand, persistent noise in y drives the walker away from strip and, consequently, the diffusion slows down. In the case of $\sigma_y^2(t)$, the behavior is straightforward: anti-persistent noise in y slows down the diffusion while persistent noise enhances it [see Fig. 4(b)]. In order to quantify the role of long-range correlations in y on $\sigma_x^2(t)$ and $\sigma_y^2(t)$, we have evaluated the dependence of the power-law exponents α_x and α_y on h_y. In Fig. 4(c), we observe a monotonic but nonlinear decay of α_x as h_y increases, while in Fig. 4(d), we confirm the straightforward behavior of α_y

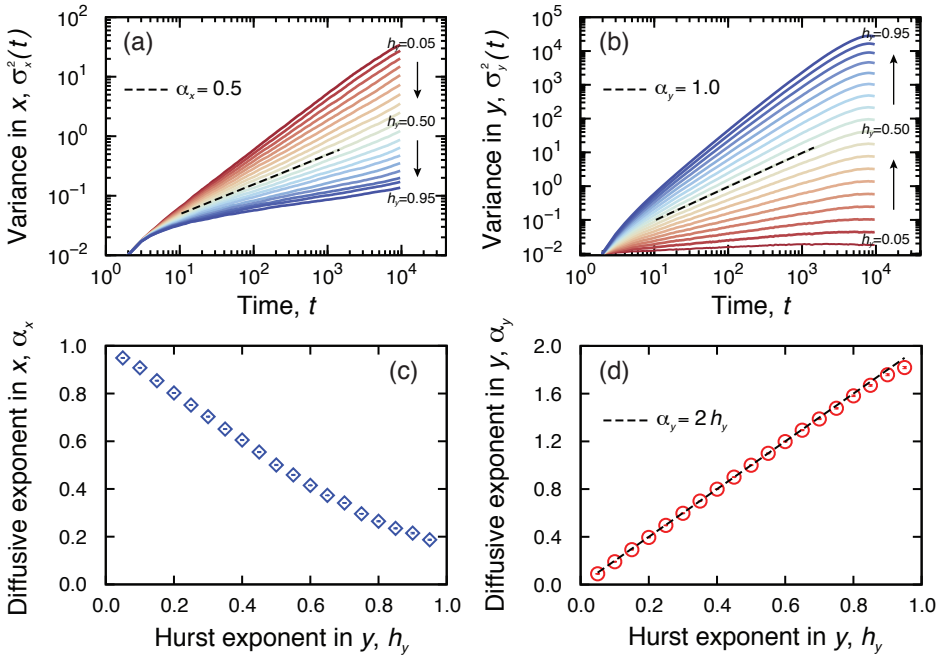

Figure 4. (color online) The role of the long-range correlated noise in the y–direction on the variances $\sigma_x^2(t)$ and $\sigma_y^2(t)$. Profile of (a) $\sigma_x^2(t)$ and (b) $\sigma_y^2(t)$ for nineteen values of h_y homogeneously distributed between 0.05 and 0.95. In both cases, the dashes lines represent the behavior of the usual comb: $\sigma_x^2(t) \sim t^{\alpha_x}$ with $\alpha_x = 0.5$ and $\sigma_y^2(t) \sim t^{\alpha_y}$ with $\alpha_y = 1$. Here, we have omitted the finite-size-like effect on the variances for better visualization of the power-law behavior. For $\sigma_x^2(t)$, we observe that the diffusion is enhanced (when compared with the usual comb) for an anti-persistent noise in y ($h_y < 0.5$) and that is slows down when the noise in y is persistent. In the case of $\sigma_y^2(t)$, anti-persistent noise slows down the diffusion while persistent noise enhances it. In (c) and (d), we show the dependence of α_x and α_y on h_y. The values of α_x and α_y were obtained by least squares fitting a linear model to the log-log relationships between the variances and the time t. The error bars (which are very tiny) are the standard errors of α_x and α_y. When adjusting the data, we have selected only the values $\sigma_x^2(t)$ and $\sigma_y^2(t)$ within the interval $30 \leq t \leq 1600$ in order to avoid the initial transient regime and the finite-size-like effect. We note the monotonic but nonlinear decay of α_x in function of h_y and the straightforward behavior of α_y versus h_y described by $\alpha_y = 2h_y$ (dashed line).

as function of h_y ($\alpha_y = 2h_y$).

Another interesting question is whether the combinations of long-range correlated noises in the x and y directions affect the diffusive behaviors in a nontrivial way. To answer this question, we have built an ensemble of 10^5 particle positions for each possible pair of h_x and h_y homogeneously distributed between 0.05 and 0.95 with step size of 0.05. For each combination of h_x and h_y, we calculate the profile of the variances $\sigma_x^2(t)$ and $\sigma_y^2(t)$ and also the power-law exponents α_x and α_y describing the main tendency of these curves (by using the same procedure of Fig. 4). Figure 5(a) shows a contour plot of α_x as a function of h_x and h_y and Fig. 5(b) represents the same for α_y. For the Fig. 5(a), we note a quite rich diffusive scenery where, depending on the values of

h_x and h_y, we may have subdiffusion slower ($\alpha_x < 0.5$) or faster ($0.5 < \alpha_x < 1$) than the usual comb, usual diffusion ($\alpha_x = 1$) and even superdiffusion ($\alpha_x > 1$). We further observe from this figure that α_x cannot be written as a linear combination of h_x and h_y (which would be represented by straight lines in this plot) and thus, the correlations in x and y present a nontrivial interplay in the behavior of α_x. On the other hand, the case of Fig 5(b) is rather simple because the correlations in x do not affect the diffusive behavior in the y–direction, this becomes evident by noting that the level curves of α_y are horizontal straight lines.

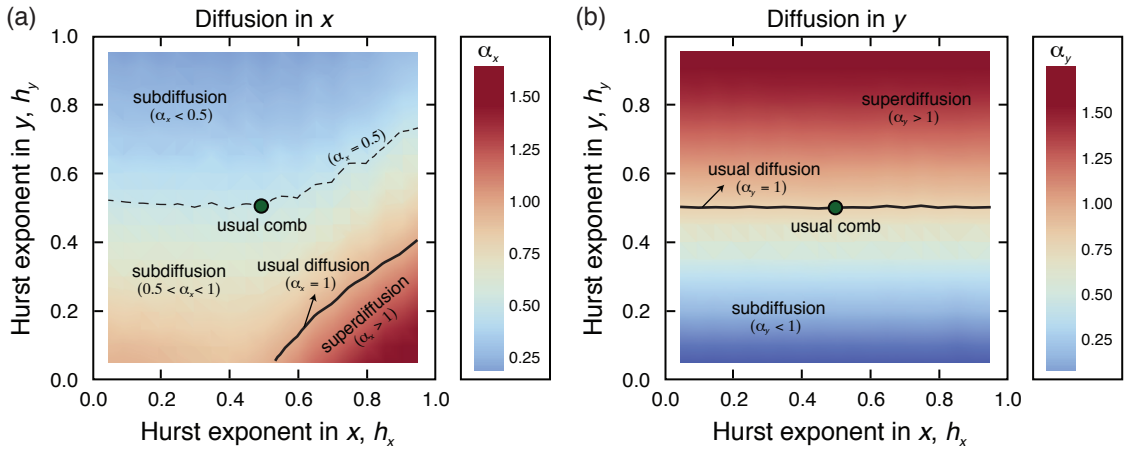

Figure 5. (color online) The interplay between the long-range correlated noises in the x and y directions on the variances $\sigma_x^2(t)$ and $\sigma_y^2(t)$. Contour plots of (a) α_x and (b) α_y as a function of h_x and h_y. We note the rich diffusive scenery in the x–direction where we may have subdiffusion slower ($\alpha_x < 0.5$) or faster ($0.5 < \alpha_x < 1$) than the usual comb, usual diffusion ($\alpha_x = 1$) and even superdiffusion ($\alpha_x > 1$). We further observe that the power-law exponent α_x cannot be expressed as a linear combination of h_x and h_y, suggesting a more complex coupling between the Hurst exponents and diffusion in the x–direction.

It is also important to investigate whether the long-range correlations affect the distribution profiles of the particle positions. In order to do so, we first calculate the marginal distributions $P(\xi_x)$ and $P(\xi_y)$ for there different values of h_y (0.05, 0.50 and 0.95) and keeping $h_x = 0.50$. Figures 6(a) and 6(b) show these distributions. We note that the distribution $P(\xi_x)$ displays tails longer than those of usual comb (dark shaded region) when the noise in the y–direction is persistent ($h_y = 0.95$) whereas, for anti-persistent noise ($h_y = 0.05$), the tails are shorter than those of usual comb and close to the Gaussian distribution (light shaded region). The distributions $P(\xi_y)$ of the normalized positions ξ_y are not affected by long-range correlated noises in the y–direction. We thus confirm that the long-range correlations in y have influence on the profiles of $P(\xi_x)$. For a better and quantitative characterization of the role of the correlated noise $\eta_y(t)$ on the shape of $P(\xi_x)$, we evaluate the coefficient of kurtosis $\kappa_x = \langle \xi_x^4 \rangle / \langle \xi_x^2 \rangle^2$ in function of h_x and h_y. For $\kappa_x > 3$ the distribution is leptokurtic (peaked) while for $\kappa_x < 3$ the distribution is platykurtic (flat) also, $\kappa_x = 3$ for a Gaussian distribution and $\kappa_x \approx 4.71$

for the usual comb (distribution of the Eq. 5). Figure 6(c) shows a contour plot of κ_x as a function of h_x and h_y, where we observe that the kurtosis ranges from very close to 3 ($\kappa_x = 3.04 \pm 0.04$ for $h_x = h_y = 0.05$) up to almost 13 ($\kappa_x = 12.55 \pm 0.87$ for $h_x = h_y = 0.95$). It is worth noting that, similar to the variance case [Fig. 5(a)], the kurtosis κ_x is not a trivial combination of h_x and h_y.

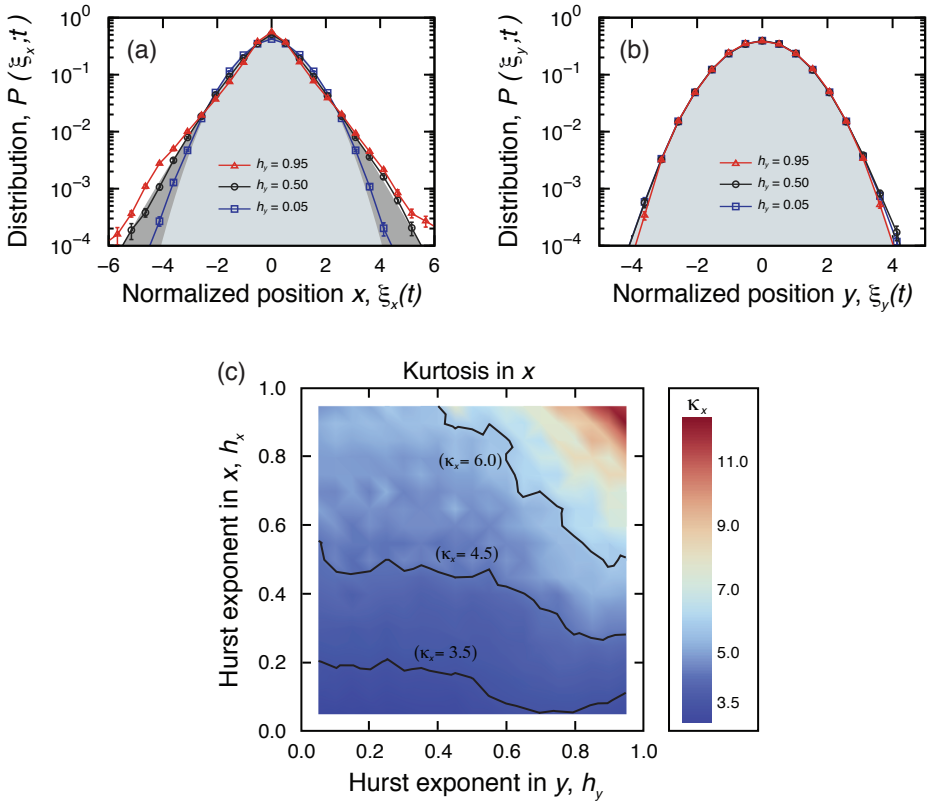

Figure 6. (color online) The effect of the long-range correlated noises on the marginal distributions. Marginal distributions of normalized positions (a) $P(\xi_x)$ and (b) $P(\xi_y)$ for there values of h_y (indicated in the plots) and $h_x = 0.5$. In both plots, the light shaded regions represent a standard Gaussian, while the dark shaded region in (a) is the profile of the marginal distribution for ξ_x of the usual comb [Eq. (5)]. For $P(\xi_x)$, we note that the distribution tails decay slower than those of usual comb when the noise in the y–direction is persistent ($h_y = 0.95$); whereas for anti-persistent noise ($h_y = 0.05$), the tails decay faster and approach the Gaussian distribution. In the case $P(\xi_y)$, the long-range correlations in y have practically no effect on the profile of these distributions. (c) Contour plot of the coefficient of kurtosis $\kappa_x = \langle \xi_x^4 \rangle / \langle \xi_x^2 \rangle^2$ for the normalized position ξ_x as a function of h_x and h_y. The value of κ_x is an average over t within the interval $30 \leq t \leq 1600$. We note that, depending on the values of h_x and h_y, the distribution $P(\xi_x)$ exhibits different profiles, which can be mesokurtic ($\kappa_x = 3$, as in the Gaussian case), leptokurtic ($\kappa_x > 3$) or platykurtic ($\kappa_x < 3$). We also observe that, similarly to variance case, κ_x cannot be expressed in terms of linear combination of h_x and h_y.

3. Summary and Conclusions

We have proposed an extension for the comb model via Langevin equations driven by long-range correlated noises (fractional Gaussian noises). We initially showed that our Langevin equations are equivalent to the generalized diffusion equation (describing the usual comb) through the comparison of the numerical-obtained variances and marginal distributions with the analytical results predicted by the diffusion equation. Next, we have presented an extensive characterization of the diffusive properties of the particle positions in function of the Hurst exponents h_x and h_y defining the correlated noises. Our results show that the noise in the $y-$direction affects the variances and marginal distributions along the $x-$direction. Specifically, long-range persistence in y slows down the diffusion in x by reducing the power-law exponent α_x and makes the tails of the marginal distribution $P(\xi_x)$ longer as $h_y > 0.5$ increases; whereas long-range anti-persistence in y enhances the diffusion in x by increasing the value of α_x and makes the tails of $P(\xi_x)$ shorter as $h_y < 0.5$ decreases. We have also investigated the interplay between the long-range correlations in the x and y directions, where we found that both α_x and the kurtosis coefficient κ_x of $P(\xi_x)$ are not a trivial (such as a linear combination) function of h_x and h_y, but instead our results suggest a more complex coupling between the Hurst exponents and the diffusion in the $x-$direction. In summary, a quite rich diffusive scenery emerges from our model which may be directly applied for describing (at least in a first approximation) some of the recent empirical findings related to diffusion in complex systems such as living cells. Furthermore, our model combines and allows the study/analysis of the interplay between different mechanisms of anomalous diffusion, geometric constraints and long-range correlations, an important fact that had not been explored within the comb model framework and that may provide a better understanding of these processes as a combination of different mechanisms.

Acknowledgments

We are all grateful to Capes, CNPq and Fundação Araucária for financial support.

References

[1] Klafter J and Sokolov I M 2005 Phys. World **18** 29
[2] Mandelbrot B B and van Ness J W 1968 SIAM Rev. **10** 422
[3] Gripenberg G and Norros I 1996 J. Appl. Probab. **33** 400
[4] Bouchad J-P and Georges A 1990 Phys. Rep. **195** 127
[5] Metzler R and Klafter J 2000 Phys. Rep. **339** 1
[6] White S R and Barma M 1984 J. Phys. A **17** 2995
[7] Ben-Avraham D and Havlin S 2000 *Diffusion and Reactions in Fractals and Disordered Systems* (Cambridge University Press, Cambridge)
[8] Weiss G H and Havlin S 1986 Physica A **134** 474
[9] Baskin E and Iomin A 2004 Phys. Rev. Lett. **93** 120603
[10] Arkhincheev V E 2007 Chaos **17** 043102
[11] Iomin A 2011 Phys. Rev. E **83** 052106

[12] Tateishi A A, Lenzi E K, Ribeiro H V, Evangelista L R, Mendes R S and da Silva LR 2011 J. Stat. Mech P02022
[13] Villamaina D, Sarracino A, Gradenigo G, Puglisi A and Vulpiani A 2011 J. Stat. Mech L01002
[14] Tateishi A A, Michels F S, dos Santos M A F, Lenzi E K and Ribeiro H V 2013 J. Stat. Mech P09017
[15] Lenzi E K, da Silva L R, Tateishi A A, Lenzi M K and Ribeiro H V 2013 Phys. Rev. E **87** 012121
[16] Iomin A 2006 Phys. Rev. E **73** 061918
[17] Iomin A 2005 J. Phys.: Conf. Ser. **7** 57
[18] Mendez V and Iomin A 2013 Chaos Solitons Fract. **53** 46
[19] Iomin A 2012 Phys. Rev. E **86** 032101
[20] Sagi Y, Brook M, Almog I and Davidson N (2012) Phys. Rev. Lett. **108** 093002
[21] Höfling F and Franosch T 2013 Rep. Prog. Phys. **76** 046602
[22] Condamin S, Tejedor V, Voituriez R, Bénichou O and Klafter J 2008 Proc. Natl. Acad. Sci. USA **105** 5675
[23] Selhuber-Unkel C, Yde P, Berg-Sørensen K and Oddershede L B 2009 Phys. Biol. **6** 025015
[24] Jeon J-H, Tejedor V, Burov S, Barkai E, Selhuber-Unkel C, Berg-Sørensen K, Oddershede L and Metzler R 2011 Phys. Rev. Lett. **106** 048103
[25] Burov S, Jeon J-H, Metzler R, and Barkai E 2011 Phys. Chem. Chem. Phys. **13** 1800
[26] Sokolov I M 2012 Soft Matter **8** 9043
[27] Leijnse N, Jeon J-H, Loft S, Metzler R and Oddershede L B 2012 Eur. Phys. J. Special Topics **204** 75
[28] Cherstvy A G, Chechkin A V and Metzler R 2013 New J. Phys. **15** 083039
[29] Brackley C A, Cates M E and Marenduzzo D 2013 Phys. Rev. Lett. **111** 108101
[30] Girst S, Hable V, Drexler G A, Greubel C, Siebenwirth C, Haum M, Friedl A A and Dollinger G 2013 Sci. Rep. **3** 2511
[31] Tabei S M A, Burov S, Kim H Y, Kuznetsov A, Huynh T, Jureller J, Philipson L H, Dinner A R and Scherer N F 2013 Proc. Natl. Acad. Sci. USA **110** 4911
[32] Cherstvy A G, Chechkin A V and Metzler R 2014 Soft Matter **10** 1591
[33] Braüchle C, Lamb C D and Michaelis J (eds.) 2010 *Single Particle Tracking and Single Molecule Energy Transfer* (Wiley-VCH, Weinheim)
[34] Weiss M 2013 Phys. Rev. E **88** 010101(R)
[35] Yamamoto E, Akimoto T, Yasui M and Yasuoka K (2014) Sci. Rep. **4** 4720
[36] Arkhincheev V E and Baskin E M 1991 Zh. Eksp. Teor. Fiz. **100** 292 [1991 Sov. Phys. JETP **73** 161].
[37] Hosking J R M 1984 Water Resour. Res. **20** 1898
[38] Arkhincheev V E 1999 JETP **88** 710
[39] da Silva L R, Tateishi A A, Lenzi M K, Lenzi E K and da Silva P C 2009 Braz. J. Phys. **39** 483